encit 2022

ABCM Associação Brasileira de Engenharia e Ciências Mecânicas

19th Brazilian Congress of Thermal Sciences and Engineering
November 6th–10th, 2022, Bento Gonçalves - RS - Brazil

ENC-2022-0010
LOCOMOTION OF AN INTRUDER WITHIN GRANULAR MEDIA

Douglas Daniel de Carvalho
Erick de Moraes Franklin
School of Mechanical Engineering, UNICAMP - University of Campinas, Rua Mendeleyev, 200, Campinas, SP, Brazil
douglascarvalho47@gmail.com; franklin@fem.unicamp.br

Abstract. *From the movement of animals and machines over and within granular matter (snakes, worms and tanks) to the penetration and collision of solid objects in the sand (space probes landing on other planets and cratering), the displacement of a solid body (intruder) within a granular medium is ubiquitous in nature. We performed discrete numerical simulations of cylindrical intruders (disks) pulled at a constant velocity amid a two-dimensional set of smaller disks, confined in a rectangular cell. By varying some of the parameters involved, we obtained the instantaneous forces and contact networks, noting that the drag experienced by the intruder is approximately constant regardless of its velocity when moving at constant speed. Furthermore, we verified that contact networks percolate forces from the intruder towards the walls, being responsible for jammed regions (which, in some cases, can lead to the complete stop of the intruder's motion) and high values of the experienced drag force. We also observed a cooperative behavior when a set of intruders is moved amid the smaller grains. Part of this work can be found in Carvalho et al., Phys. Rev. E, 2022.*

Keywords: *granular matter, granular flows, force chains, DEM simulations*

1. INTRODUCTION

From the movement of animals and machines over and within granular matter (snakes, worms and tanks) to the penetration and collision of solid objects in the sand (space probes landing on other planets and cratering), the displacement of a solid body (intruder) within a granular medium is ubiquitous in nature (Askari and Kamrin, 2016; Zheng *et al.*, 2018). When in motion, the intruder may experience different phenomena, such as the dissipation of its kinetic energy through the generated collisions in the grains (Bester and Behringer, 2017), jamming (Candelier and Dauchot, 2009), and stick-slip dynamics (Kozlowski *et al.*, 2019; Carlevaro *et al.*, 2020).

One important aspect of granular media is the formation of forces and stresses networks (force chains) under the action of external applied stresses. Because granular matter is a discrete medium, inter-particle forces are transmitted via a history-dependent contact network, which then forms an inhomogeneous distribution of filamentary force chains (Majmudar and Behringer, 2005). Such forces are only transmitted through the inter-particle contacts, which leads to a strong anisotropic distribution of stresses (Radjai *et al.*, 1998). Understanding these forces and their spatial correlations is one of the main goals of granular mechanics, since it is important for understanding jamming, shear-induced yielding and mechanical response in these materials (Majmudar and Behringer, 2005).

When intruders are set in motion in granular media, the force networks generated along the intruder-granular interface rapidly fluctuate in space and time (Clark *et al.*, 2014), as this movement leads to local reorganizations of the granular packing (Kolb *et al.*, 2013), causing either breakage or formation of chains around it. This generates a strongly oscillating drag force on the intruder (Kolb *et al.*, 2013; Seguin *et al.*, 2016; Carvalho *et al.*, 2022) and, in some cases, may lead to creeping (Candelier and Dauchot, 2009) and to the formation of jammed regions, which can bring the intruder to a complete stop.

Some works focused on the motion of an intruder being pulled at a constant velocity amid smaller grains (Kolb *et al.*, 2013; Seguin *et al.*, 2016; Kozlowski *et al.*, 2019; Carlevaro *et al.*, 2020; Carvalho *et al.*, 2022). In particular, for the case of a single intruder, Kolb *et al.* (2013) and Seguin *et al.* (2016) found that as the intruder is displaced, the regions in front of it tend to compact, further leading to a recirculation of grains that form a dynamic arc right behind it. In addition, the formation of an empty cavity behind the intruder as it moves has also been reported. We recently investigated numerically the displacement of a steel intruder amidst a two-dimensional granular pack (Carvalho *et al.*, 2022). Among other findings, we have shown that contact networks can be divided into two types: (i) a bearing network, which carries forces greater than the average contact force, that percolates from the intruder towards the walls, and (ii) a dissipative network, which carries weaker forces smaller than the average contact force. We also showed that these chains break due to creeping,

that the cavity formed behind the intruder tends to decrease as the grain packing fraction increases, and that basal friction plays an important role in grain dynamics (Carvalho *et al.*, 2022).

The case of a group of intruders moving through grains was substantially less studied and, in most studies, the intruders moved vertically through a less dense granular packing (Pacheco-Vázquez and Ruiz-Suárez, 2010; Solano-Altamirano *et al.*, 2013; Kawabata *et al.*, 2020). Of special interest is the groundbreaking work of Pacheco-Vázquez and Ruiz-Suárez (2010), who investigated the impact of sets of intruders on a less dense granular system, showing the existence of a cooperative dynamics between intruders never before observed in granular experiments. The authors showed that the intruders moved collectively, in order to provoke changes in the movement dynamics (drag experienced), leading to more efficient motions (Pacheco-Vázquez and Ruiz-Suárez, 2010).

Although studied beforehand, the physics behind the dynamics of these motions still remains poorly understood and important issues remain to be further investigated. To this end, this work consists of numerical simulations of cylindrical intruders (disks) pulled at a constant velocity in a two-dimensional assembly of smaller bidisperse disks in a rectangular confining cell, so that the intruder(s) and the grains have relative displacements. The simulations are carried out with the discrete element method (DEM) using the open source software LIGGGHTS. We present quantitative measurements of the force experienced by the intruder(s) in different physical configurations. In addition, we show that, for the case when two intruders are moved collectively, there exists an optimal separation between them that leads to a smaller drag experienced. It is important to note that parts of this communication are present in Carvalho *et al.* (2022) and Carvalho and Franklin (2022).

2. METHODOLOGY

2.1 Numerical setup

The numerical simulations consist in pulling intruders (solid disks) into a two-dimensional assembly of smaller disks. The $d_{int} = 16$ mm diameter and $h_{int} = 3.6$ mm high steel intruders are pulled at a constant velocity ($10^{-1} \leq V_0 \leq 10$ mm/s) amid a granular assemble of a bidisperse mixture of photoelastic polyurethane (PSM-4) disks with small diameter $d_s = 4$ mm and large diameter $d_l = 5$ mm, in order to prevent crystallization (Speedy, 1999). The disks with height $h_g = 3.2$ mm are distributed in a proportion of $N_l/N_s \approx 0.64$, where N_s and N_l are the number of small and large particles, respectively, in a way that the area occupied by the small and large grains in the simulation cell is almost the same. For the case with a single intruder, $N_s = 4832$ and $N_l = 3092$, and for the case of two intruders, $N_s = 4826$ and $N_l = 3089$. The disks are placed over a horizontal glass plate and are enclosed in a glass square area of $L_x \times L_y = 400 \times 400$ mm^2. All simulations are done within a fixed cell size, in a way that the initial packing fraction of the model is kept constant at $\phi_0 = 0.76$. The physical properties of the materials used in the numerical simulations are summarized in Tab. (1).

Table 1: Physical properties of all materials used in the numerical simulations.

	Material	**Young's modulus [Pa]**	**Poisson's ratio**	**Density [kg/m^3]**	**Size [mm]**
Intruder	Steel[(1)]	1.96×10^9	0.29	7800	$d_{int} = 16$
Grains	Polyurethane[(1),(2)]	4.14×10^6	0.50	1280	d_s = 4; d_l = 5
Walls	Glass[(1)]	0.64×10^{11}	0.23	2500	L_x = 400; L_y = 400

(1) Hashemnia and Spelt (2014)

(2) Gloss (2000)

Although Young's modulus of steel is $E = 1.96 \times 10^{11}$ Pa, we considered a smaller value in the numerical simulations of $E = 1.96 \times 10^9$ Pa to avoid prohibitive timesteps, without giving up the accuracy of the results (Lommen *et al.*, 2014). Since we consider pure two-dimensional simulations, no motion of both grains and intruder in the direction perpendicular to the plane xy is considered (Fig. (1a)). The intruder is initially placed in the granular medium at the left side of the simulation cell at $(x_i, y_i) = (-160, 0)$ and is pulled at a constant velocity V_0 from left to right towards its final position $(x_f, y_f) = (160, 0)$, according to the schemes presented in Fig. (1a). For the case with the displacement of two intruders, they are initially placed at the same longitudinal coordinate but the transverse position of the intruders is varied, the two being separated by a distance Δy, as indicated in Fig. (1b). The time evolution of the drag force F_D exerted by the grains onto the intruder disk during its displacement, the forces in each grain as well as their displacements are computed every time-step. In addition, to avoid any possible boundary effects in the force results, the analyzed cell area is restricted to a central square region of interest (ROI) - green-dashed area in Fig. (1a) - of size $A_{ROI} = 160 \times 160$ mm^2. The physical conditions used in the numerical simulations are very similar to the ones used in the experiments performed by Seguin *et al.* (2016).

After determining the physical configuration to be studied, the set of particles with the aimed proportion is generated. First, the particles are randomly distributed over a space larger than the wanted computational domain. Then, the computational domain is compressed to its final size so that the desired packing fraction ϕ is achieved, according to Eq. (1), for

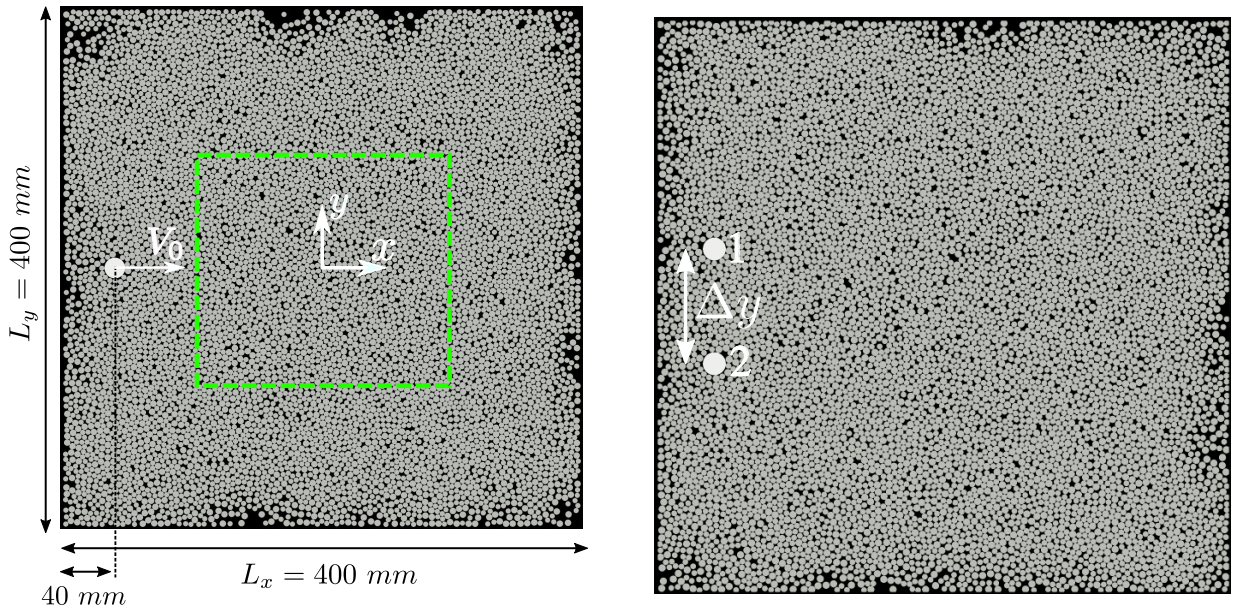

(a) (b)

Figure 1: (a) Numerical setup for one intruder. (b) Numerical setup for the case of two intruders. Credits for (a): Carvalho *et al.* (2022). Credits for (b): Carvalho and Franklin (2022).

N_i intruders:

$$\phi = \frac{\frac{\pi}{4}(N_s d_s^2 + N_l d_l^2)}{L_x L_y - N_i(\frac{\pi}{4} d_{int}^2)} \tag{1}$$

The particles are then allowed to relax for a sufficient time until no substantial degree of kinetic energy is attained. Once the fully relaxed state is reached, the intruder is set in motion at a constant velocity.

2.2 Discrete element method (DEM)

The simulations were carried out using LIGGGHTS (LAMMPS Improved for General Granular and Granular Heat Transfer Simulations) (Kloss *et al.*, 2012), which is a discrete element method (DEM) open source software for modelling granular flows. In conjunction with LIGGGHTS, we made use of the two-dimensional Discrete-Element bonded-particle Sea Ice model - DESIgn toolbox (Herman, 2016).

For the case of N disk-shaped grains, each with a constant mass $m_i = \rho_i h_i \pi r_i^2$ for $i = 1 \cdots N$, their motion can only be influenced by: (i) the particle-particle and particle-wall interaction forces, and (ii) other external forces. For simplicity, the particle-wall forces will not be included in the equations below, since they are modeled in the exact same way as the particle-particle interactions. For each particle $j \in N$ in contact with particle i, there exists a contact force $\mathbf{F}_{c,ij}$ which is conveniently expressed as the sum of two components, normal $\mathbf{F}_{c,ij,n}$ and tangential $\mathbf{F}_{c,ij,t}$ to the plane of contact. The normal component contributes to the translational motion of disks i and j and the tangential component the their rotational motion. This way, the torque $\mathbf{M}_{c,ij}$ due to the tangential forces may be expressed as (Herman, 2016):

$$\mathbf{M}_{c,ij} = \mathbf{r}_{ij} \times \mathbf{F}_{c,ij,t}, \tag{2}$$

where $\mathbf{r}_{ij}$ is a vector pointing from the center of disk i with center position vector $\mathbf{x}_i = (x_i, y_i, z_i = 0)$ to the contact point with disk j. Once again, it is important to mention that this is a two-dimensional problem, which precisely means that $z_i = 0$.

The motion of all grains is governed by Newton's second law of motion. Therefore, the translational and rotational motions of particle i, in contact with grains $j \in \mathcal{C}$, where $\mathcal{C}$ denotes all particles in contact with grain i, are given by:

$$m_i \frac{d\mathbf{u}_i}{dt} = \sum_{j \in \mathcal{C}} \mathbf{F}_{c,ij} + \mathbf{F}_e, \tag{3}$$

where t denotes time, $\mathbf{u}_i = (u_{x,i}, u_{y,i}, u_{z,i} = 0)$ is the velocity vector of particle i, and $\mathbf{F}_e$ is the sum of all external forces acting on particle i, and,

$$I_{z,i} \frac{d\omega_{z,i}}{dt} = M_{c,ij} + M_e, \tag{4}$$

where $I_{z,i} = (1/2)m_i r_i^2$ is the moment of inertia, $\omega_{z,i}$ is the angular velocity of particle i, $M_{c,ij}$ is the net moment generated by the tangential contact forces and M_e is the net moment of the external forces.

Although there are no explicit external forces acting on our system, since we are dealing with dry granular media, the DESIgn toolbox does not consider the sliding frictional force that exists between the grains/intruder and the bottom glass wall on which they are placed. Therefore, we had to implement a new force to account for the effects of an effective solid friction between the grains/intruder and the base into the library of the DESIgn toolbox. This force was modeled in a similar manner to what has been done in Carlevaro *et al.* (2020). In short, if a grain i is moving at a certain velocity $v_i = |\mathbf{u}_i|$ above a threshold v' ($v_i > v'$), then a dynamic friction force with the bottom wall is considered and equal to $F_d = -\mu_{d,g} m_i g \mathbf{u}_i/|\mathbf{u}_i|$. Conversely, if it is moving with a velocity v_i smaller than or equal to the threshold v' ($v_i \leq v'$), then an static friction force with the bottom wall $F_s = -\mu_{s,g} m_i g \mathbf{u}_i/|\mathbf{u}_i|$ is applied and the particle is immobilized by setting $v_i = 0$. This ensures that a grain will only resume its motion if the forces exerted by the other grains exceed the static friction force (Carlevaro *et al.*, 2020). In this model, we do not consider rotational friction forces between the grains and the bottom wall.

As for modeling the contact forces, the nonlinear elastic Hertz-Mindlin contact model, appropriate for non-cohesive interactions, is used (Di Renzo and Di Maio, 2005). Parameters regarding contact interactions and physical properties of the materials involved are required in this model. The parameters used in our simulations are summarized in Tab. (2).

Table 2: Coefficients used in the numerical simulations.

Coefficient	**Symbol**	**Base value**
Friction coefficient (grain-grain)[(1)]	μ_{gg}	1.2
Friction coefficient (grain-intruder)[(2)]	μ_{gi}	1.8
Friction coefficient (grain-wall)[(1)]	μ_{gw}	0.4
Restitution coefficient (grain-grain)	ϵ_{gg}	0.3
Restitution coefficient (grain-intruder)[(2)]	ϵ_{gi}	0.7
Restitution coefficient (grain-wall)[(3)]	ϵ_{gw}	0.7
Dynamic friction coefficient (grain-bottom wall)[(1)]	$\mu_{d,g}$	0.4
Static friction coefficient (grain-bottom wall)	$\mu_{s,g}$	0.7
Dynamic friction coefficient (intruder-bottom wall)	$\mu_{d,i}$	0.7
Threshold velocity (dynamic/static friction)	v'	5.0×10^{-4}

(1) Carlevaro *et al.* (2020)

(2) Hashemnia and Spelt (2014)

(3) Gondret *et al.* (2002)

All of our simulations were performed with a time step $\Delta t = 3.2 \times 10^{-6}$ s, which, in the worst scenario, is less than 10% of the Rayleigh time (Derakhshani *et al.*, 2015). For more details regarding the numerical setup, please refer to Carvalho *et al.* (2022).

3. RESULTS AND DISCUSSION

We first present the results for a single intruder being pulled at constant velocity, as in Fig. (1a) and afterwards we present results for two intruders pulled at constant velocity, according to Fig. (1b).

3.1 Single intruder case

For all simulated conditions, the resultant force on the intruder was calculated at each time step. We will refer to it as the instantaneous drag force on the intruder $F_D = |\boldsymbol{F}_D|$. We also obtained, for each different condition, the time-averaged magnitude $\langle F_D \rangle$.

Figure 2a presents F_D as a function of time t when the intruder moves with V_0 = 2.7 mm/s in a system with mean packing fraction ϕ = 0.76. An initial transient is present, associated with the beginning of the intruder's motion followed by an increase in F_D due to an increasing number of contacts. After some time, the mean value of F_D remains roughly constant, however with very high oscillations with peaks that reach as much as three times the mean value. As shown in (Carvalho *et al.*, 2022), those strong oscillations are caused by the formation and breaking of contact networks that are responsible for percolating forces within the the smaller grains. We should mention that the same behavior was found experimentally by Seguin *et al.* (2016) and Kolb *et al.* (2013): an increase in F_D while the bearing chains persist followed by a fast decrease when these chains break.

Figure 2b shows the time-averaged magnitude of the drag force $\langle F_D \rangle$ as a function of the intruder velocity V_0 for ϕ = 0.76. We observe that the values obtained are roughly independent of V_0 (as in Seguin *et al.* (2016) and Seguin *et al.* (2013)), with a mean value $\langle F_D \rangle \approx 0.21$. For the exact same case, Seguin *et al.* (2016) found experimentally $\langle F_D \rangle \approx$

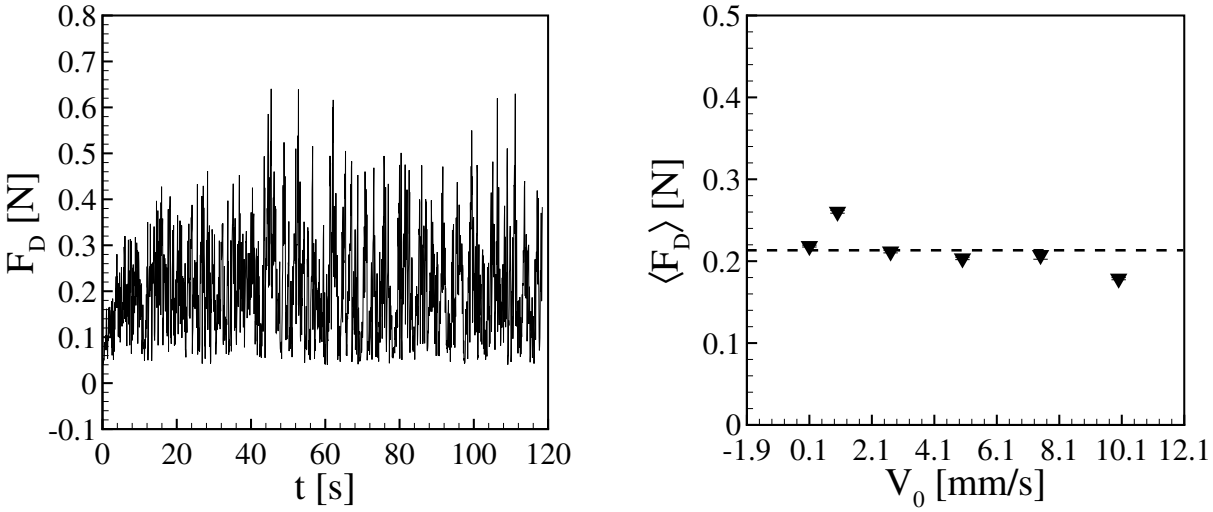

(a) (b)

Figure 2: (a) Magnitude of the resultant force on the intruder F_D for V_0 = 2.7 mm/s as a function of time t. (b) Time-averaged magnitude of the resultant force on the intruder $\langle F_D \rangle$ as a function of its velocity. Credits for (a) and (b): Carvalho *et al.* (2022).

0.22. Considering that one may expect experimental uncertainties in Seguin *et al.* (2016) and that most of the materials properties (with the exception of the diameter) were obtained from other works (as indicated in Tab. (1)), the agreement is quite good. These results are remarkable as they not only validate our numerical routine but also indicate the non-dependence of the intruder's drag on its velocity, since in granular materials friction is more related to contact than to inertia.

3.2 Two intruders case

As for the case with a single intruder, the instantaneous drag force $\boldsymbol{F}_D$ was computed at each time step, as well as its time-averaged magnitude F_D for different vertical separations Δy (as indicated in Fig. (1b)). We afterward computed an average value for both intruders, $\langle F_D \rangle_{mean}$, by simply adding their time averages F_D and dividing by two.

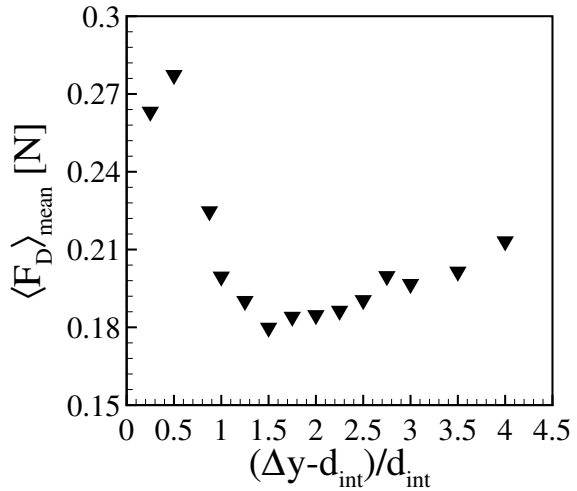

Figure 3: Magnitude of the average resultant force on both intruders $\langle F_D \rangle_{mean}$ as a function of their initial vertical separation Δy normalized by the intruder diameter d_{int}. Credits: Carvalho and Franklin (2022).

Figure (3) shows $\langle F_D \rangle_{mean}$ as a function of $(\Delta y - d_{int})/d_{int}$, which corresponds to the spacing between the surfaces of the intruders normalized by their diameter. It is clear that a non-monotonic variation is present, with a decrease in the average drag force for $(\Delta y - d_{int})/d_{int}$ < 1.5 as the separation between intruders increases, and an increasing trend for $(\Delta y - d_{int})/d_{int}$ > 1.5. This way, there is an optimal distance D_{opt} that results in minimum average drag when the normalized separation between them is 1.5 ($D_{opt} \rightarrow \Delta y = 2.5 d_{int}$). We should also note that, in the vicinities of this optimal separation the drag acting on each intruder is approximately 0.18 N, which corresponds to 85% of the value

for a single intruder shown above (0.21 N) for the same velocity and packing fraction. Furthermore, there is a range $1 \leq (\Delta y - d_{int})/d_{int} \leq 3.5$ in which $\langle F_D \rangle_{mean}$ is smaller than the drag for a single intruder, indicating that some type of cooperative dynamics between the intruders is taking action within the granular system, similar to that presented by Pacheco-Vázquez and Ruiz-Suárez (2010). This can be useful for designing devices that agitate soil or other granular surfaces.

4. CONCLUSIONS

We numerically investigated the forces on a two-dimensional granular system displaced by intruders moving with constant velocity. We used the DEM open source LIGGGHTS (Kloss *et al.*, 2012) together with the DESIgn toolbox (Herman, 2016). For the case of a single intruder displacing the granular medium, we varied its velocity and showed that the resultant force on it is approximately independent of its velocity and that the oscillations present in its time force signal are associated with the formation and breaking of contact networks. As for the case of two intruders displacing the granular medium, we showed that there is a cooperative behavior between them, as well as the existence of an optimal separation to not only achieve minimum drag, but also reduce the drag compared to the case of a single intruder.

5. ACKNOWLEDGEMENTS

The authors are grateful to FAPESP (Grant numbers 2018/14981-7 and 2020/04151-7) for the financial support provided. The authors would like to thank Nicolao Cerqueira Lima and Fernando David Cúñez Benalcázar for their physical discussions about this work.

6. REFERENCES

Askari, H. and Kamrin, K., 2016. "Intrusion rheology in grains and other flowable materials". *Nature materials*, Vol. 15, No. 12, pp. 1274–1279.

Bester, C.S. and Behringer, R.P., 2017. "Collisional model of energy dissipation in three-dimensional granular impact". *Physical Review E*, Vol. 95, No. 3, p. 032906.

Candelier, R. and Dauchot, O., 2009. "Creep motion of an intruder within a granular glass close to jamming". *Physical review letters*, Vol. 103, No. 12, p. 128001.

Carlevaro, C.M., Kozlowski, R., Pugnaloni, L.A., Zheng, H., Socolar, J.E. and Kondic, L., 2020. "Intruder in a two-dimensional granular system: Effects of dynamic and static basal friction on stick-slip and clogging dynamics". *Physical Review E*, Vol. 101, No. 1, p. 012909.

Carvalho, D.D. and Franklin, E.M., 2022. "Collaborative behavior of intruders moving amid grains". *Manuscript submitted for publication*.

Carvalho, D.D., Lima, N.C. and Franklin, E.M., 2022. "Contacts, motion, and chain breaking in a two-dimensional granular system displaced by an intruder". *Physical Review E*, Vol. 105, No. 3, p. 034903.

Clark, A.H., Petersen, A.J. and Behringer, R.P., 2014. "Collisional model for granular impact dynamics". *Physical review E*, Vol. 89, No. 1, p. 012201.

Derakhshani, S.M., Schott, D.L. and Lodewijks, G., 2015. "Micro–macro properties of quartz sand: experimental investigation and dem simulation". *Powder Technology*, Vol. 269, pp. 127–138.

Di Renzo, A. and Di Maio, F.P., 2005. "An improved integral non-linear model for the contact of particles in distinct element simulations". *Chemical engineering science*, Vol. 60, No. 5, pp. 1303–1312.

Gloss, K.T., 2000. *A Photoelastic Investigation Into The Effects Of Cracks And Boundary Conditions On Stress Intensity Factors In Bonded Specimens*. Ph.D. thesis, Virginia Tech.

Gondret, P., Lance, M. and Petit, L., 2002. "Bouncing motion of spherical particles in fluids". *Physics of fluids*, Vol. 14, No. 2, pp. 643–652.

Hashemnia, K. and Spelt, J.K., 2014. "Particle impact velocities in a vibrationally fluidized granular flow: measurements and discrete element predictions". *Chemical Engineering Science*, Vol. 109, pp. 123–135.

Herman, A., 2016. "Discrete-element bonded-particle sea ice model DESIgn, version 1.3 a–model description and implementation". *Geoscientific Model Development*, Vol. 9, No. 3, pp. 1219–1241.

Kawabata, D., Yoshida, M., Shimosaka, A. and Shirakawa, Y., 2020. "Discrete element method simulation analysis of the generation mechanism of cooperative behavior of disks falling in a low-density particle bed". *Advanced Powder Technology*, Vol. 31, No. 4, pp. 1381–1390.

Kloss, C., Goniva, C., Hager, A., Amberger, S. and Pirker, S., 2012. "Models, algorithms and validation for opensource DEM and CFD–DEM". *Progress in Computational Fluid Dynamics, an International Journal*, Vol. 12, No. 2-3, pp. 140–152.

Kolb, E., Cixous, P., Gaudouen, N. and Darnige, T., 2013. "Rigid intruder inside a two-dimensional dense granular flow: Drag force and cavity formation". *Physical Review E*, Vol. 87, No. 3, p. 032207.

Kozlowski, R., Carlevaro, C.M., Daniels, K.E., Kondic, L., Pugnaloni, L.A., Socolar, J.E., Zheng, H. and Behringer, R.P., 2019. "Dynamics of a grain-scale intruder in a two-dimensional granular medium with and without basal friction". *Physical Review E*, Vol. 100, No. 3, p. 032905.

Lommen, S., Schott, D. and Lodewijks, G., 2014. "DEM speedup: Stiffness effects on behavior of bulk material". *Particuology*, Vol. 12, pp. 107–112.

Majmudar, T.S. and Behringer, R.P., 2005. "Contact force measurements and stress-induced anisotropy in granular materials". *Nature*, Vol. 435, No. 7045, pp. 1079–1082.

Pacheco-Vázquez, F. and Ruiz-Suárez, J., 2010. "Cooperative dynamics in the penetration of a group of intruders in a granular medium". *Nature communications*, Vol. 1, No. 1, pp. 1–7.

Radjai, F., Wolf, D.E., Jean, M. and Moreau, J.J., 1998. "Bimodal character of stress transmission in granular packings". *Physical review letters*, Vol. 80, No. 1, p. 61.

Seguin, A., Bertho, Y., Martinez, F., Crassous, J. and Gondret, P., 2013. "Experimental velocity fields and forces for a cylinder penetrating into a granular medium". *Physical Review E*, Vol. 87, No. 1, p. 012201.

Seguin, A., Coulais, C., Martinez, F., Bertho, Y. and Gondret, P., 2016. "Local rheological measurements in the granular flow around an intruder". *Physical Review E*, Vol. 93, No. 1, p. 012904.

Solano-Altamirano, J., Caballero-Robledo, G., Pacheco-Vázquez, F., Kamphorst, V. and Ruiz-Suárez, J., 2013. "Flow-mediated coupling on projectiles falling within a superlight granular medium". *Physical Review E*, Vol. 88, No. 3, p. 032206.

Speedy, R.J., 1999. "Glass transition in hard disc mixtures". *The Journal of chemical physics*, Vol. 110, No. 9, pp. 4559–4565.

Zheng, H., Wang, D., Chen, D.Z., Wang, M. and Behringer, R.P., 2018. "Intruder friction effects on granular impact dynamics". *Physical Review E*, Vol. 98, No. 3, p. 032904.

7. RESPONSIBILITY NOTICE

The authors are solely responsible for the printed material included in this paper.